

## The mechanical design of nacre

By A. P. JACKSON<sup>†</sup>, J. F. V. VINCENT<sup>1</sup> AND R. M. TURNER<sup>2</sup>

<sup>1</sup> Biomechanics Group, Department of Pure and Applied Zoology, The University, Whiteknights, P.O. Box 228, Reading RG6 2AJ, U.K.

<sup>2</sup> ICI plc, Wilton Materials Research Centre, P.O. Box 90, Wilton, Middlesborough TS6 8JE, U.K.

(Communicated by R. M. Alexander, F.R.S. – Received 22 January 1988  
– Revised 6 May 1988)

[Plate 1]

Mother-of-pearl (nacre) is a platelet-reinforced composite, highly filled with calcium carbonate (aragonite). The Young modulus, determined from beams of a span-to-depth ratio of no less than 15 (a necessary precaution), is of the order of 70 GPa (dry) and 60 GPa (wet), much higher than previously recorded values. These values can be derived from ‘shear-lag’ models developed for platey composites, suggesting that nacre is a near-ideal material. The tensile strength of nacre is of the order of 170 MPa (dry) and 140 MPa (wet), values which are best modelled assuming that pull-out of the platelets is the main mode of failure. In three-point bending, depending on the span-to-depth ratio and degree of hydration, the work to fracture across the platelets varies from 350 to 1240 J m<sup>-2</sup>. In general, the effect of water is to increase the ductility of nacre and increase the toughness almost tenfold by the associated introduction of plastic work. The pull-out model is sufficient to account for the toughness of dry nacre, but accounts for only a third of the toughness of wet nacre. The additional contribution probably comes from debonding within the thin layer of matrix material. Electron microscopy reveals that the ductility of wet nacre is caused by cohesive fracture along platelet lamellae at right angles to the main crack. The matrix appears to be well bonded to the lamellae, enabling the matrix to be stretched across the delamination cracks without breaking, thereby sustaining a force across a wider crack. Such a mechanism also explains why toughness is dependent on the span-to-depth ratio of the test piece. With this last observation as a possible exception, nacre does not employ any really novel mechanisms to achieve its mechanical properties. It is simply ‘well made’.

The importance of nacre to the mollusc depends both on the material and the size of the shell. Catastrophic failure will be very likely in whole, undamaged shells which behave like unnotched beams at large span-to-depth ratios. This tendency is increased by the fact that predators act as ‘soft’ machines and store strain energy which can be fed into the material very quickly once the fracture stress has been reached. It may therefore be advantageous to have a shell made of an intrinsically less tough material which is better at stopping cracks (e.g. crossed lamellar).

† Present address: Smith & Nephew Research Ltd, Gilston Park, Harlow CM20 2RQ, U.K.

However, nacre may still be preferred for the short, thick shells of young molluscs, as these have a low span-to-depth ratio and can make better use of ductility mechanisms.

## INTRODUCTION

Nacre is one of several different kinds of molluscan shell material. Each is essentially a two-phase composite of calcium carbonate (as calcite or aragonite) with an organic matrix containing glycine- and alanine-rich protein and polysaccharide (Currey 1980). Much interest has centred on the organic matrix of these shell materials with the aim of deducing their involvement in the process of biomineralization (see, for example, Weiner & Traub 1981; Krampitz *et al.* 1983; Greenfield *et al.* 1984; Addadi & Weiner 1985). The fact that some shell materials contain far more matrix than is needed to deposit calcium carbonate successfully suggests that the role of the matrix is more than simply to nucleate and organize the crystallites. In addition, it is likely to be responsible for determining the mechanical properties of the whole shell, first through its intrinsic properties and, second, by controlling such mechanically significant features as size, shape and distribution of the brittle crystallites (Wainwright *et al.* 1976).

Considered as a composite material, nacre is filled with 95% (by volume) calcium carbonate (in the form of aragonite) in a matrix of protein and polysaccharide. This is a remarkably high filler content compared with man-made composites: the mechanical behaviour of such composites had been predicted but rarely, if ever, observed. With such a high proportion of ceramic the material should be brittle, yet nacre has a work of fracture about 3000 times greater than that of pure ceramic.

Nacre is a composite reinforced with platelets rather than with fibres, an arrangement not commonly found in man-made composites. Each polygonal tablet of aragonite interlocks perfectly with its neighbour to form sheets which are stacked on top of each other in a staggered formation. No platelet composite has been made with such small platelets in such perfect alignment and distribution.

We describe here the measurement and modelling of three mechanical properties – the Young modulus, tensile strength and fracture toughness – of nacre.

## MATERIALS AND METHODS

### General

All tests were done on nacre from the shell of a bivalve mollusc, *Pinctada*. It was supplied from three sources: a banjo maker from Penzance (as variously shaped 1 mm thick offcuts); W. Gillott & Son of Sheffield (as 35 mm diameter discs, 0.3–3 mm thick); and Eaton's Rock Shop, London (as strips 1.5 mm × 50 mm × 25 mm). Only the white variety was used (cf. Currey 1977). The specimens were large, flat and free of growth lines which have been shown to act as planes of weakness (Jackson 1986; Srinivasan 1941).

The samples were machined with a piercing saw, a diamond circular saw, a polishing burr and carborundum paper. Some nacre was tested dry (stored at

ambient temperature and humidity) and some was tested wet (having been soaked in distilled water for three weeks). The water content at saturation was 0.2% of the total mass of wet nacre, half of which is present in 'dry' nacre (Jackson 1986).

The samples were tested mechanically with a table model Instron 4202 at a cross-head speed of 0.5 mm min<sup>-1</sup> and the output recorded on a BBC Goerz chart recorder. Nomenclature for the direction of movement of the cross-head or plane of crack propagation follows that of Currey (1977), namely either 'across', 'along' or 'between' the platelets.

### Microscopy

Specimens of nacre were polished with jeweller's rouge and notched with an engraver in the 'across' direction before being fractured in three-point bending either stably (allowing the crack to arrest mid-way) or unstably. These were coated with gold and examined in a Hitachi S520 scanning electron microscope (SEM) at a magnification of  $\times 10000$ .

Fracture surfaces of nacre cleaved in the 'between' direction were examined with a Hitachi S800 SEM. This machine has a field emission gun, giving a resolution of 15 nm at 1 kV and a maximum magnification of  $\times 150000$ . To check that the particles of evaporated gold were not responsible for the obvious features at such high magnification, a control specimen with no metallic or carbon coating was inspected under the same conditions, a procedure possible only at this low accelerating voltage.

### The Young modulus

Samples of nacre were prepared with approximate dimensions 5 mm  $\times$  1.5 mm  $\times$  40 mm for 'across' and 1.8 mm  $\times$  0.8 mm  $\times$  35 mm for the 'along' test pieces, to an accuracy of  $\pm 0.1$  mm. Most specimens were tested in three-point bending at a span (*S*) to depth (*D*) ratio of 20, but some from each category were also tested at smaller *S/D* ratios by progressively decreasing the span for the same beam. Fatigue effects were discounted by taking three types of precaution: (i) successive tests were done leaving five minutes between each; (ii) the beams were loaded to the same force, not the same displacement, so the stress did not increase dramatically with increase in *S/D*; and (iii) at the largest span, the beam was loaded many times at five-minute intervals yet no change in the Young modulus was observed. Thus the strains imposed were insufficient to cause fatigue effects.

The moduli were subsequently corrected for the effect of machine compliance by using the formula

$$(P/x)_{\text{corr}} = (P/x)_{\text{app}} / \{ [1 - (P/x)_{\text{app}}] / [(P/x)_{\text{machine}}] \},$$

where  $(P/x)$  is the slope of the load-deflection curve (Wagner *et al.* 1981).

The machine compliance was obtained by lowering the cross-head onto a tall piece of steel of negligible compliance mounted on the three-point bending apparatus.

### Tensile strength

Dumbbell shapes were cut from thick (1–2 mm) discs of nacre with a diamond circular saw. A smooth transition from the wide ends to the parallel central strip was achieved by careful abrasion with carborundum paper and polishing with an 'Alundum'-impregnated rubber burr (Dentsply Ltd). A 3 mm hole was drilled through the centre of each end-tag to accommodate a steel pin. These pins also located through holes on the Instron load cell and base attachments. Only those specimens that broke in the central parallel region were included in the results.

### Fracture toughness

Toughness is not the easiest property to measure in biological materials owing to their tendency to contravene certain assumptions made in current fracture theory; e.g. the requirement of zero plasticity in linear elastic fracture mechanics. Toughness was measured in three different ways.

#### *Single-edge-notched, three-point bending, unstable fracture*

Rectangular beams were prepared of cross-sectional dimensions 0.5–2.0 mm × 2–6 mm (depth × width) and of varying length according to the required span. Single edge notches (SEN) were machined with a 30° sharp engraving cutter. These notches were further sharpened with a razor blade; both the tip radius (0.1 mm) and the depth ( $a$ ) of the notch were measured with a calibrated microscope. Notches were varied in depth from  $a/D = 0.05$  to  $a/D = 0.6$ . In 'between' nacre, small (1.5 mm × 2 mm × 2 mm) blocks were notched with a piercing saw, the notches sharpened with a razor and the blocks glued by their large faces to two brass beams.

Test pieces were loaded to failure in the three-point bending rig at  $S/D$  ratios of 16 and 4 for 'across' nacre, 10 and 4 for 'along' nacre and 4 for 'between' nacre. Work areas were measured from the chart-recorder curves by using a Summagraphics Bit Pad One connected to a Hewlett-Packard 85 computer. For uncontrolled fracture this is the area under the force-displacement curve up to peak load but not beyond ( $= U_{\text{init}}$ ).

The strain energy stored in the machine was measured by driving the cross-head down on to a negligibly compliant block of steel mounted on the three-point bending test rig. From the resulting calibration curve, work areas were measured at load increments of 5 N, thus allowing the strain energy in the machine to be calculated at any given load by interpolation. The appropriate machine strain energy ( $U_{\text{mach}}$ ) at the failure load of the test piece was subtracted from the initial failure energy ( $U_{\text{init}}$ ) to give the stored strain energy of the test piece ( $U_s$ ). The critical stress intensity factor ( $K_c$ ) of each test piece was calculated as follows:

$$K_c = (3P_{\max} SYa^{0.5})/(2BD^2),$$

where  $Y$  is the sum between 4 and 0 of  $A_n(A/D)^n$  such that

	$A_0$	$A_1$	$A_2$	$A_3$	$A_4$
$S/D = 16$	1.99	-2.47	12.97	-23.17	24.80,
$S/D = 8$	1.96	-2.75	13.66	-23.98	25.22,
$S/D = 4$	1.93	-3.07	14.53	-25.11	25.80

(Brown & Srawley 1966), and where the other symbols are as defined previously. The polynomial coefficients at intermediate  $S/D$  ratios were interpolated linearly.

The critical strain energy release rate ( $G_c$ ) was calculated from  $G_c = U_3/(BD\phi)$ , where  $\phi = \{[Y^2(a/D)d(a/D)]/(Y^2a/D)\} + [(S/18D)Y^2(a/D)]$  (Williams 1984) and  $Y$  is as defined above for any  $S/D$  ratio. The factor  $\phi$  corrects for the excess strain energy stored in the specimen which does not go into producing new fracture surfaces. The presence of such excess energy is caused by the geometry of the test, the three-point bending configuration being particularly susceptible to unstable fracture (Williams 1984).

#### *Single-edge-notched three-point bending, stable fracture*

Dimensions of test pieces were the same as for unstable fracture tests except that notches were introduced with piercing saw (and sharpened with a razor) to a relative depth ranging from  $a/D = 0.6$  to  $a/D = 0.8$ . An  $S/D$  ratio of 4 was chosen for all tests to facilitate stable cracking. 'Between' fracture could not be investigated owing to the difficulty of cutting sufficiently deep notches in the nacre without prematurely cleaving it. Values for  $K_c$  were not derived owing to the inaccuracy of the finite-width correction factors above  $a/D = 0.6$  (Brown & Srawley 1966).

One experiment consisted of allowing the crack to propagate continuously until the load had dropped to zero. The total fracture energy ( $U_2$ ) – calculated from the whole area under the force–displacement curve – was divided by the ligament area to obtain a slow propagation  $G_c$ , otherwise represented by  $R$ , i.e.

$$R = G_c = U_2/B(D-a).$$

No correction for machine strain energy was needed.

In another experiment the fracture process was interrupted at intervals by unloading the specimen and then reloading. How far the crack had propagated each time was monitored *in situ* with a calibrated microscope. This time several values for  $R$  under slow propagation could be derived from each test-piece from the formula

$$R = G_c = U_{2(\text{seg})}/B(a_1 - a_0),$$

where  $U_{2(\text{seg})}$  is the segmental fracture work area enclosed by adjacent loading lines, and  $a_1 - a_0$  is the difference between the starting crack length and the crack length after unloading.

#### *Single-edge-notched, tensile, unstable fracture*

Dumb-bell-shaped test pieces were notched in the 'across' or 'along' platelet direction halfway down their length. Relative notch depths were varied from  $a/W = 0.05$  to  $a/W = 0.6$ . The test pieces were pin loaded and tested to failure,  $K_c$  being calculated from

$$K_c = P_{\max} Ya^{0.5}/Bw,$$

where  $Y = 1.99 - 0.40(a/W) + 18.7(a/W)^2 - 38.48(a/W)^3 + 53.85(a/W)^4$ , irrespective of  $L/W$  ratio (Brown & Srawley 1966).

If displacement is taken from cross-head movement in unstable, tensile fracture,

reliable values for  $G_c$  or  $R$  cannot be obtained because an unknown amount of deformation occurs at the joints. Consequently no attempt was made to measure  $G_c$ .

#### *Interfacial shear strength*

Interfacial shear strength ( $\tau_i$ ) is needed for theoretical modelling of tensile strength. Dry or wet nacre was tested to failure in three-point bending at an  $S/D$  ratio of about 3. The beams were orientated in the 'across' fracture direction so that the interlaminar shear strength between adjacent platelet lamellae was tested. This was calculated from

$$\tau_i = 3P_{\max}/4BD$$

(American Society for Testing and Materials 1976).

#### *Shear modulus of the organic matrix*

To model the Young modulus of nacre it is necessary to have an estimate of the shear modulus of the organic matrix. Direct tests on chemically extracted matrix cannot supply the required information, partly because the network will be denatured and partly because the matrix *in situ* is constrained by the surrounding ceramic. Such constraint will increase the actual modulus as it exists in the intact composite.

An alternative method is to test nacre in a particular geometry wherein the only shear forces present are those tending to slide adjacent lamellae apart from each other. Such a geometry is to be found in the three-point bend test. On decreasing the  $S/D$  ratio of a beam in three-point bending the interlaminar shear stresses increase and the central vertical deflection of the beam becomes a mixture of that due to bending and that due to shear. The shear deflection is given by

$$Y_s = 3PS/10MBD,$$

where  $M$  is the interlaminar shear modulus (Stephens 1970), and the apparent Young modulus of nacre may be expressed as

$$E_{\text{app}} = PS^3/4BD^3(y_b + y_s),$$

where  $y_b$  is the vertical deflection due to bending and  $y_s$  is the vertical deflection due to shear. Substituting for  $y_s$  in this equation and rearranging, we have

$$(1/E_{\text{app}}) = (1/E_{\text{real}}) + (6/5M)(D/S)^2.$$

Thus by measuring the apparent Young modulus at a range of  $S/D$  ratios the interlaminar shear modulus can be estimated. Assuming that the individual lamellae do not deflect very much in shear, we can say that the interlaminar shear modulus is also equivalent to the constrained shear modulus of the organic matrix.

## RESULTS AND DISCUSSION

#### *The Young modulus*

##### *Experimental*

Load-deflection curves were generally linear for dry nacre but showed a shoulder at high strain with wet nacre, indicative of plastic yield (cf. Currey 1977). When-

ever the trace was curved the modulus was calculated from the tangent to the initial slope.

Suitable  $S/D$  ratios, chosen to avoid shear, have been recommended for various materials including metals (8), timber (24) (Roark & Young 1975), and fibre-reinforced composites (60) (Zweben *et al.* 1979), but none has been given for nacre. Lest it be doubted how drastic is the effect of insufficient  $S/D$ , Zweben *et al.* (1979) showed that for a unidirectional Kevlar-polyester composite, the use of  $S/D = 16$  instead of 60 causes a drop in the measured modulus to about 65% of its true value!

Plots of apparent Young modulus against  $S/D$  ratio (figure 1) show that a safe  $S/D$  for nacre is 15 or more. Without correction for machine compliance the fall-off with decreasing  $S/D$  is even more pronounced.

By using an  $S/D$  of about 20 and correcting for machine compliance, the data presented in table 1 can reliably be said to be true flexural Young moduli: they are all very high. Even the smallest value of 60 GPa for 'along, wet' nacre exceeds Currey & Taylor's (1974) average for *Pinctada* by about 25 GPa. Currey & Taylor quote an  $S/D$  ratio of 10.25 which will give an underestimate of  $E$  (based on figure 1) of 7 GPa. Currey & Brear (1984) quote moduli for *Pinctada* in agreement with those obtained here.

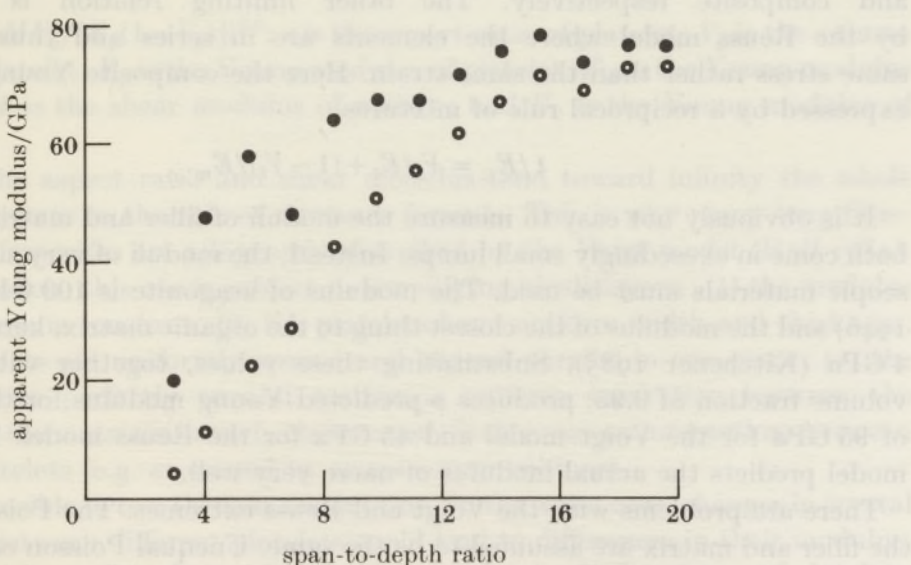


FIGURE 1. The effect of span-to-depth ratio on the apparent Young modulus ( $E$ ) of 'across, wet' nacre. Open circles are before, and closed circles after, correction for machine compliance.

The effect of water is to reduce the modulus by about 10 GPa. The differences are highly significant ('across':  $d = 4.349$ ,  $0.0001 > p > 0.00001$ ; 'along':  $t(35 \text{ d.f.}) = 3.027$ ,  $0.01 > p > 0.001$ ). In contrast to many biological materials, where the plasticizing effect of water is to reduce the stiffness considerably, nacre is only slightly affected; presumably because of its limited capacity for water retention.

There is no significant difference between moduli in the 'across' and 'along' directions.

TABLE 1. THE YOUNG MODULUS OF *PINCTADA NACRE*  
(For 'across' orientation,  $S/D = 20$ ; for 'along',  $S/D = 35$ .)

	mean corrected Young modulus	standard deviation	number of tests
	GPa	GPa	
across, dry	73	9	35
across, wet	64	8	35
along, dry	70	11	19
along, wet	60	10	18

### Theoretical modelling

The usual starting point for the prediction of the Young modulus of a composite is to treat the filler and matrix as forming one of two possible relations with each other. In the first (Voigt) model the elements are in parallel with each other and undergo the same strain. The Young modulus of the composite is then given by

$$E_C = V_f E_f + (1 - V_f) E_m,$$

where  $V$ ,  $E$ ,  $f$ ,  $m$  and  $C$  stand for volume fraction, Young modulus, filler, matrix and composite respectively. The other limiting relation is represented by the Reuss model where the elements are in series and thus receive the same stress rather than the same strain. Here the composite Young modulus is expressed by a reciprocal rule of mixtures

$$1/E_C = V_f/E_f + (1 - V_f)/E_m.$$

It is obviously not easy to measure the moduli of filler and matrix in nacre as both come in exceedingly small lumps. Instead, the moduli of very similar macroscopic materials must be used. The modulus of aragonite is 100 GPa (Hearmon 1946) and the modulus of the closest thing to the organic matrix, keratin, is about 4 GPa (Kitchener 1985). Substituting these values, together with a platelet volume fraction of 0.95, produces a predicted Young modulus for the composite of 95 GPa for the Voigt model and 45 GPa for the Reuss model. Thus neither model predicts the actual modulus of nacre very well.

There are problems with the Voigt and Reuss extremes. The Poisson ratios of the filler and matrix are assumed to be the same. Unequal Poisson contraction of the components within the composite can cause additional elastic constraints with the result that the Voigt model – normally an upper bound model – becomes a lower bound model instead (Harris 1980). There are, of course, improvements and modifications of the simple Voigt and Reuss extremes but, like the Hirsch model, they are only semi-empirical (McGee & McCullough 1981). Neither model takes into account the distribution of stress along the length of a filler particle. For a composite containing spherical filler particles or randomly orientated particles of any shape this is a negligible consideration, but for a perfectly aligned platelet composite such as nacre it could cause a substantial reduction of the observed modulus. This may be explained as follows. A single platelet is embedded in organic

matrix and load is transferred from matrix to the platelet by shear forces at the matrix–platelet interface. For a matrix of finite shear modulus, the tensile stress in the platelets will build up from each end and, if the platelet is long enough, will reach a plateau somewhere in the central region of the platelet. The longer the platelet is in relation to its thickness, the smaller will be the proportion of its length which is wasted in carrying loads well below its load-carrying potential. At very large aspect ratios, when the build up of stress is negligible, the average strains along the platelet and matrix are equal and the modulus is governed simply by the rule of mixtures or the Voigt model. Conversely, with platelets of very small aspect ratio a significant proportion of the platelet is under-loaded and the surrounding matrix has to strain by a large amount to achieve relatively little strain in the platelet. The result is a much larger overall strain than is to be expected from the given amount of platelet filler material, thus the composite modulus is reduced.

The way in which the aspect ratio and Young modulus of the filler and the shear modulus of the matrix affect the rule-of-mixtures Young modulus was derived by Cox in his ‘shear lag’ analysis for fibre-reinforced composites (Cox 1952). A similar analysis has been developed for platelet composites by Padawer & Beecher (1970)

$$E_C = V_p E_p [1 - (\tanh(u)/u)] + (1 - V_p) E_m,$$

where  $u = s \{MV_p/[E_p(1 - V_p)]\}^{0.5}$ ;  $s$  is the aspect ratio of platelet;  $V_p$  is the volume fraction of platelet;  $E_p$  is the Young modulus of platelet;  $E_m$  is the Young modulus of matrix;  $M$  is the shear modulus of matrix; and  $E_C$  is the Young modulus of composite.

Thus as the aspect ratio and shear modulus tend toward infinity the whole expression reverts to the rule-of-mixtures formula. This is why many long-fibre-reinforced composites are adequately described by the Voigt model (Hull 1981).

Like all models, this one is subject to simplifying idealizations: (1) the modulus of the platelets is constant; (2) the platelets have uniform width and thickness; (3) the platelets are uniformly spaced and aligned parallel in one plane; (4) the matrix adheres perfectly to and maintains uniform separation between the platelets; (5) the matrix is linearly elastic; and (6) there are no interactions between adjacent platelets (e.g. as caused by stress concentrations).

It is not possible to test the first assumption. In the worst case, changes in crystal orientation between different platelets could lead to differences in their modulus, but the effect is small and would probably cancel out over large areas of platelets. *Pinctada* nacre has very regular organization of its platelets, so the second and third assumptions are satisfied. The fourth assumption has been shown to be satisfied (Jackson *et al.* 1987). Assumption five is unlikely in view of the highly strained fibrils that can be seen inside delamination cracks (Jackson *et al.* 1987) so on this point the model might need to be improved. Of all the assumptions the last one is most difficult to satisfy. In such a tightly packed composite as nacre, stress concentrations at the ends of the platelets may well be large enough to affect the Young modulus seriously. Fortunately, a modification of the Padawer–Beecher model which takes into consideration these interactions has been made by Riley

(Lusis *et al.* 1973). With  $u$  as defined previously, the composite modulus is then given by

$$E_C = V_p E_p \{[1 - \ln(u + 1)]/u\} + (1 - V_p) E_m.$$

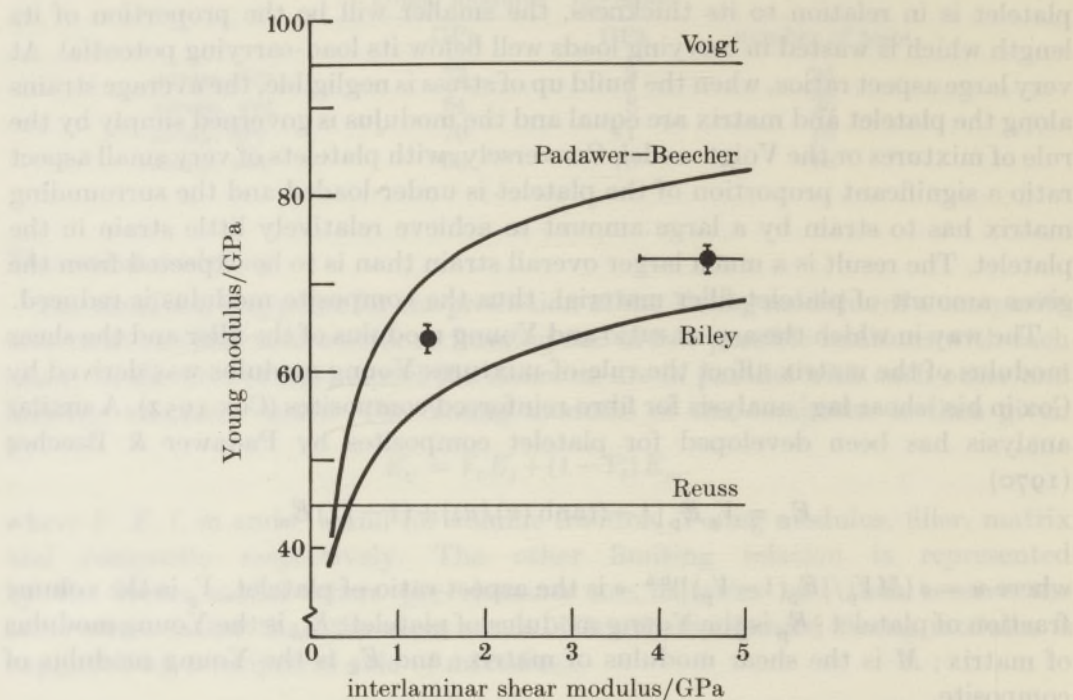


FIGURE 2. Theoretical predictions of the Young modulus of nacre at any given shear modulus of the organic matrix. The experimentally determined Young moduli of 'across, dry' (upper circle) and 'across, wet' (lower circle) lie between the two shear lag models of Padawer & Beecher and Riley. Bars represent standard errors.

The Young modulus of nacre, predicted by the Padawer-Beecher and Riley models over a wide range of shear moduli, is plotted in figure 2. The curves were calculated with  $s = 8$ ,  $E_p = 100$  GPa and  $V_m = 0.95$ , and neglecting the contribution from the matrix. Also included are the upper bound (Voigt) and lower bound (Reuss) estimates which are independent of the shear modulus of the matrix. By taking the shear modulus of dry matrix as 4.6 GPa and that of wet matrix as 1.4 GPa (Jackson 1986) and by interpolating the expected Young modulus for nacre, we find for the Padawer-Beecher model  $E_{\text{dry}} = 82$  GPa and  $E_{\text{wet}} = 72$  GPa, and for the Riley model  $E_{\text{dry}} = 68$  GPa and  $E_{\text{wet}} = 58$  GPa. The observed moduli for 'across' nacre lie in between these predictions and are somewhat closer to the Riley model than to the Padawer-Beecher model. The fact that the points exceed the Riley prediction implies that this model is a slight over-correction for the effects of platelet interaction; that they can be so high at all – compared with, say, mica composites whose moduli fall well below the Riley model (Lusis *et al.* 1973) – is an indication of the near-ideal construction of nacre as a platelet composite.

### Tensile strength

#### Experimental

Owing to the difficulty involved in their preparation, only five test pieces of dry or wet nacre were tested in tension, producing a tensile strength of  $167 \pm 22$  MPa when dry, and of  $130 \pm 24$  MPa when wet (figures are mean  $\pm$  standard deviation). Currey obtained a tensile strength for *Pinctada* nacre of 90 MPa; his largest value for tensile strength for nacre does not exceed 116 MPa (Currey 1980) which is lower than our values. We consider these high values to be more correct because, through stress-concentrations and end effects, it is easier to underestimate than overestimate tensile strength. It is, of course, possible that the exact species, origin or storage conditions of *Pinctada* nacre used by Currey are not the same as those employed here.

Dry nacre is significantly stronger than wet nacre in tension ( $t$  (8 d.f.) = 2.577,  $0.01 > p > 0.02$ ) which is the expected outcome for a material of higher modulus failing at approximately the same strain. Wet nacre yields considerably before failure when the specimen can be seen to go opaque close to the fracture surface.

#### Theoretical modelling

The tensile strength of a platelet composite is governed by a rule of mixtures in which the volume fractions are multiplied by the average stresses and not the ultimate (breaking) stresses of the components. Nacre is a special case because the volume fraction of matrix is low and we can write

$$\sigma_t = V_p \bar{\sigma}_p,$$

where:  $\bar{\sigma}_p$  is the average tensile stress in a platelet, and  $\sigma_t$  is the tensile strength of nacre, so neglecting the contribution of the matrix.

The average platelet stress may be found by considering how the tensile stress changes along the length of a platelet when it is loaded in shear through the surrounding matrix. Ideally, it should be possible to apply shear lag analysis, but the Padawer-Beecher (1970) equation for strength failed to give meaningful results. However, the simple shear transfer model of Glavinchevski & Piggott (1973) can be modified to allow for the interactions between platelets although it includes the assumption that tensile stress builds up linearly from the ends of a platelet rather than – as shear lag correctly predicts – asymptotically.

Consider an idealized square platelet, of length  $2L$  and thickness  $t$ , embedded in organic matrix. For the system to be in equilibrium, the tensile forces in the platelet must equal the shear forces at the platelet–matrix interface, i.e.

$$2Lt d\sigma_p = -2(2L dx) \tau_i,$$

where  $x$  is the distance along the length of a platelet.

The tensile stress in the platelet (it is assumed) builds up linearly from each end and reaches a maximum in the centre; conversely, the shear stress at the interface increases toward each end but is zero in the middle. As the composite is stressed more, the stress gradients – and the peak stresses – increase until either the ultimate tensile stress of the platelets or the interfacial shear strength is exceeded.

Which of these happens first depends on the strengths of the platelet and interface and on the aspect ratio of the platelet. At large aspect ratios there is enough traction on a platelet to cause the stress to level out at its breaking strength, whereas at low aspect ratios the cross-sectional area can carry enough load to cause the platelet to shear out of the matrix.

When the aspect ratio is sufficiently large, a 'plateau' stress can be calculated by moving a certain distance,  $mL$ , away from the end of the platelet. Substituting  $mL$  for  $x$  in the above equation, we have  $\sigma_{pp} = \tau_i ms$ , where  $\sigma_{pp}$  is the plateau tensile stress in a platelet;  $s$  is the aspect ratio ( $2L/t$ );  $m$  is the fraction of length occupied by changing tensile stress at the ends of a platelet; and  $\tau_i$  is the interfacial shear strength.

A critical aspect ratio ( $s_c$ ) is defined as the aspect ratio at which a plateau stress is just reached. Putting  $m = 1$  (corresponding to half the basal length of the triangle)

$$s_c = \sigma_{pp}/\tau_i.$$

It is now possible to calculate the tensile strength to be expected if the platelets break or pull out, and whether or not there is any interaction between the platelets.

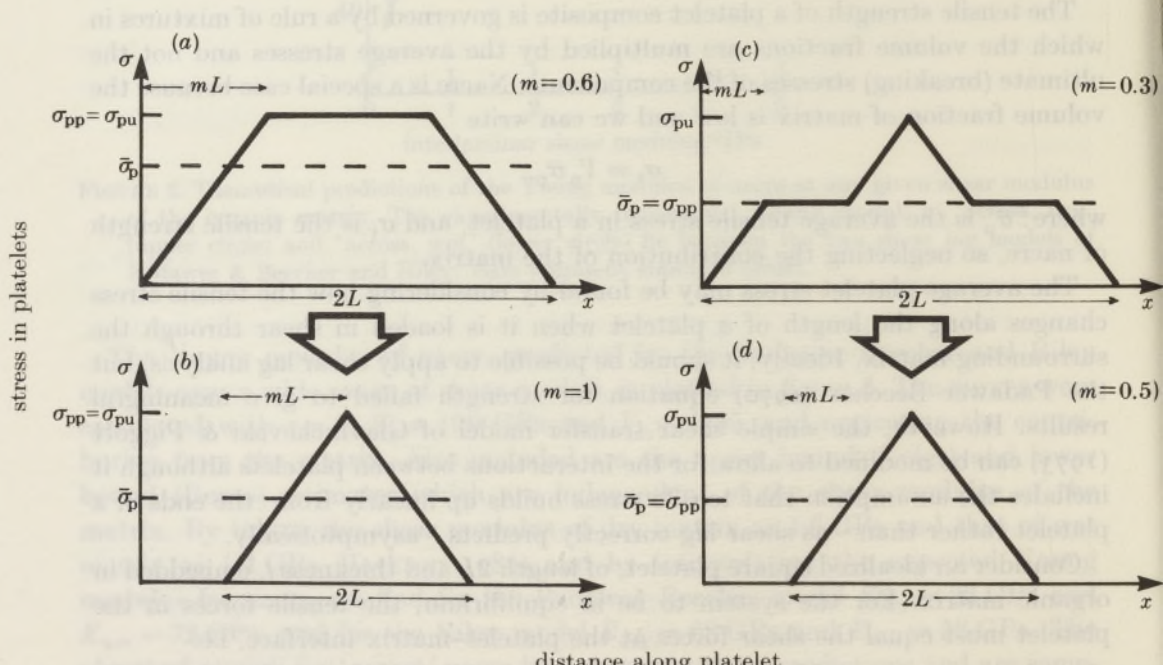


FIGURE 3. Diagram to show the build-up of tensile stress along the length of a platelet embedded in a matrix, either neglecting interactions for (a)  $s > s_c$  and for (b)  $s_c > s$ , or accounting for interactions for (c)  $s > s_c$  and for (d)  $s_c > s\delta_p$ , average stress of platelet;  $\sigma_{pp}$ , plateau stress in platelet;  $\sigma_{pu}$ , ultimate (breaking) stress of platelet;  $2L$ , length of platelet;  $m$ , proportion of length occupied by varying stress and hence the value of  $m$  in (a) and (c) is purely arbitrary. See text for fuller explanation. Adapted from Piggott (1980).

*Platelet fracture with no interactions.* The distribution of stress is illustrated in figure 3a. The average stress is obtained by dividing the area under the stress-length curve by the total length of platelet, which depends on the aspect ratio of the platelets, i.e.

$$\bar{\sigma}_p = \sigma_{pp} (1 - s_c/2s).$$

Substituting this expression into the rule of mixtures and noting that  $\sigma_{pp} = \sigma_{pu}$ , we have

$$\sigma_t = V_p \sigma_{pu} (1 - s_c/2s).$$

From this equation it can be seen that nacre will achieve 95% of the platelet strength when  $s$  is very large compared with  $s_c$ . Taking Currey's estimate for the flexural strength of aragonite as 100 MPa, it implies that the maximum attainable strength of nacre, assuming that platelets break, is only 95 MPa; at least 40 MPa lower than the observed strength.

*Platelet fracture with interactions.* To take into account the interactions between neighbouring platelets, Piggott (1980) argued (following Riley 1968; Chen & Lewis 1970) that for a 50% overlap of adjacent platelets, the tensile stress in the centre of the platelet would be elevated above its plateau level owing to the additional shear transfer from overlapping platelets immediately above. The stress distribution envisaged is shown in figure 3c. Because the area under the central spike is equal to the area under the sloping ends, the average platelet stress will be given by  $\bar{\sigma}_p = \sigma_{pp}$ , irrespective of the aspect ratio of the platelets. The plateau stress is half the maximum possible stress which, when the platelet breaks, is half the tensile strength of the platelets. Therefore,

$$\sigma_t = \frac{1}{2} V_p \sigma_{pu}.$$

The strength of nacre can now reach a maximum of only about 48 MPa – a mere 30% or so of the actual strength.

*Platelet pull-out.* When platelets pull out the tensile stress distribution is triangular. In the absence of interactions (figure 3b),  $m = 1$  and  $\sigma_{pp} = \tau_i s$ .

The average stress is half the plateau stress, so it follows that

$$\sigma_t = \frac{1}{2} V_p \tau_i s.$$

In the presence of interactions (figure 3d),  $m = 0.5$  and  $\sigma_{pp} = \tau_i s$ . But this time the average stress is the same as the plateau stress, so we arrive at the same expression for  $\sigma_t$ . Thus stress concentrations have no effect on the strength of nacre when the platelets pull out of the matrix.

Substituting the interfacial shear strengths for dry and wet nacre (Jackson 1986), for dry nacre  $\sigma_t = 175$  MPa (compared with the actual value of 167 MPa) and for wet nacre  $\sigma_t = 141$  MPa (compared with 130 MPa). Thus the pull-out model makes a very good prediction indeed. Figure 4 summarizes how the strength of nacre is dependent on  $s$ ,  $s_c$  and  $V_p \sigma_{pu}$  in the presence or absence of interactions.

The possibility that the strength of nacre is determined by a mode of failure involving platelet breakage cannot be ruled out, for we do not know the strength of a single platelet. If, as is most likely, interaction between platelets does occur,

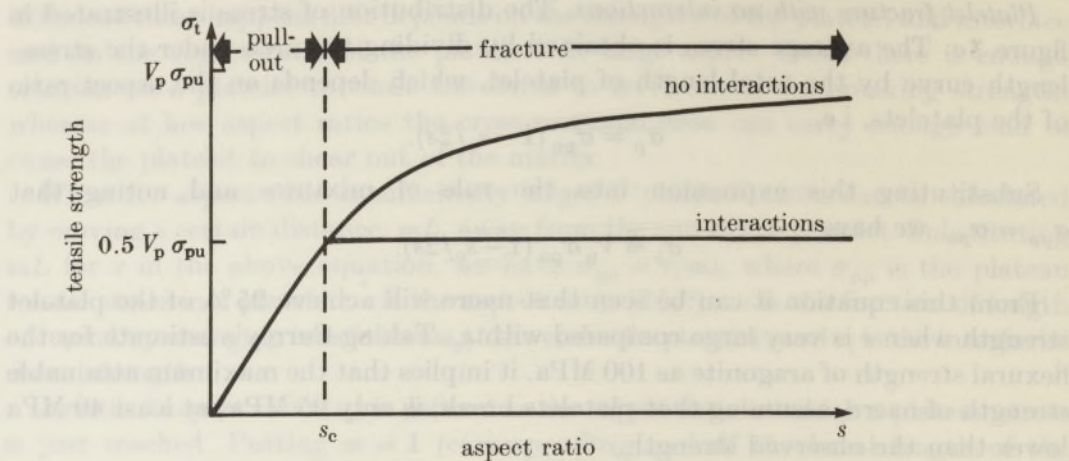


FIGURE 4. Summary of the theoretical variation of tensile strength of nacre with the aspect ratio of the platelets. At  $s < s_c$  there is pull-out and platelet interactions have no effect. At  $s > s_c$  the platelets fracture at a stress equal to half the rule-of-mixtures prediction when there are no interactions, or at a value proportional to  $(s_c/2s)$  when interactions are neglected. The full rule-of-mixtures is not realized until the aspect ratio is very large; by this time the platelets are really sheets or ribbons.

then according to this model we can predict that the strength of a single platelet is at least twice the tensile strength of nacre (i.e. more than 300 MPa).

However, the tensile strength of nacre is dependent on the interfacial shear strength, which in turn is dependent on the water content of the matrix. But only a failure strength due to pull-out is affected by the interfacial shear strength. It could still be that dehydration allows  $s_c$  to be exceeded and breakage to take place; yet pull-out would still be required to explain the decreased strength of wet nacre.

#### FRACTURE TOUGHNESS

##### *Experimental*

Results for the three different types of fracture toughness test are presented in tables 2–5.

##### *Single edge notch, three-point bending, unstable fracture*

It is clear from table 2 that, with the exception of ‘between, dry’ nacre (which is very brittle), orientation of the test piece makes very little difference to the strain energy release rates. There is a significant difference between the value for  $K_c$  in the ‘along, wet’ and ‘across, wet’ conditions but this is probably an artefact of cracking in the presence of plastic flow, as is discussed later.

Toughness is more strongly influenced by water content. At  $S/D = 4$  the  $G_c$  for wet, ‘along’, nacre is some three times that of the dry nacre. At ambient temperature and humidity nacre is 50% hydrated, therefore it was decided to desiccate a further set of samples by heating them for three days at 110 °C. These were tested in the same way and their results are included in table 2. It is clear that

TABLE 2. TOUGHNESS OF *PINCTADA* NACRE

(Results from tests in three-point bending with a single edge notch, resulting in unstable fracture, at different  $S/D$  ratios.)

	$S/D$	$G_c/(J m^{-2})$ mean $\pm$ s.d.	$n$	$K_c/(MN m^{-\frac{3}{2}})$ mean $\pm$ s.d.	$n$
across, desiccated	4	264	138	9	2.9
across, dry	16	352	130	14	4.6
	4	464	143	8	3.3
across, wet	16	587	189	14	4.5
	4	1240	778	9	3.7
along, dry	11	328	32	10	5.0
	4	439	142	9	3.7
along, wet	4	788	252	7	5.0
between, dry	4	—	—	2.1	0.3
					15

toughness is further reduced on removal of the remaining water. Interestingly, changes in toughness are not always manifested by changes in  $K_c$ ; indeed,  $K_c$  seems to be far a less sensitive measure of toughness than  $G_c$ . This is probably because  $K_c$  becomes less meaningful in the presence of ductility.

Lastly, the results show that  $G_c$  is improved at the lower  $S/D$  ratio, especially in nacre. This implies that the mechanism of energy absorption is geometry- and loading mode-dependent, for which a likely explanation is that shear stresses at small  $S/D$  cause extra work to be done in debonding adjacent platelet lamellae remote from the crack tip.

To what extent can these values be claimed to be true for  $G_c$  and  $K_c$ ; how much does plastic work contribute?

To answer the first question, the force-displacement curves were examined for nonlinearity. In the desiccated state nacre gave traces that were linear up to failure, in the dry state they were usually straight but sometimes slightly shouldered, and in the wet state each one displayed a large amount of levelling off before failure. The fact that the work areas contain plastic work and are not therefore triangular up to failure undoubtedly accounts for much of the discrepancy between the observed  $G_c$  and the  $G_c$  expected from the relation

$$K_{c(meas)}^2 = E_{(meas)} G_{c(exp)}.$$

See figure 5.

It is difficult to know how much plasticity can be tolerated before  $K_c$  measurement becomes unacceptable. An excessively large plastic zone can lead to an underestimate or an overestimate of  $K_c$ , depending on the size of certain dimensions of the test-piece. For SEN tests in three-point bending the dimensions  $B$ ,  $D$  and  $a$  must be above a certain minimum size to give a  $K_c$  independent of geometry. One criterion used for polymers and metals is that  $B$ ,  $D$  and  $a$  should not fall below a multiple of the plane stress plastic zone size, so that

$$B_{\min} = 2.50 (K_{Ic}/\sigma_Y)^2,$$

$$D_{\min} = 6.25 (K_{Ic}/\sigma_Y)^2,$$

$$a_{\min} = 2.50 (K_{Ic}/\sigma_Y)^2$$

(Hashemi & Williams 1984; Brown & Srawley 1966).

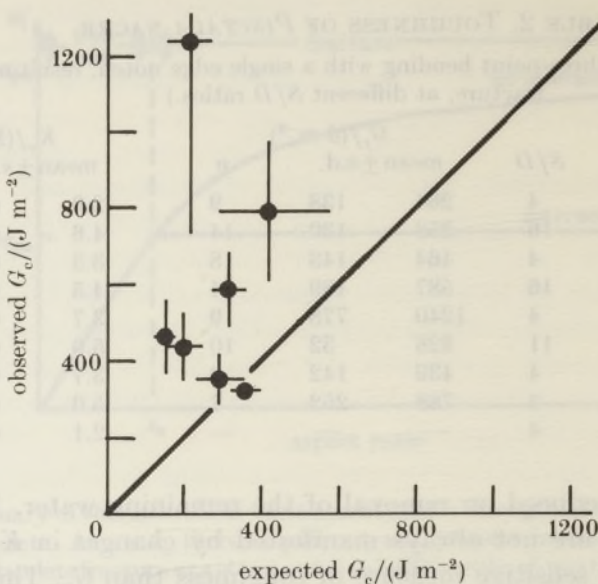


FIGURE 5. Comparison of observed and expected critical strain energy release rates predicted by the isotropic relation  $K_c^2 = EG_c$ . Bars represent 95 % confidence limits.

Enlarged plastic zones always occur where the tip of the crack meets the two sides of the specimen where there is effectively a condition of plane stress. Reducing the breadth,  $B$ , of an SEN specimen therefore increases the relative proportion of these plane-stress zones and causes an elevation of the  $K_c$  above the plane strain  $K_{Ic}$  value (Knott 1973). Insufficient depth of specimen,  $D$ , allows whatever plastic zone there is to occupy a greater proportion of the ligament area giving rise to more gross yielding before fracture. Under these conditions the plane-strain value is underestimated rather than overestimated; so the lower bound  $K_c$  is not always a  $K_{Ic}$ . This somewhat counter-intuitive result can nevertheless be predicted by the yield theory of Bilby *et al.* (1963), presented simply by Hashemi & Williams (1984). Lastly, the lower limit imposed on crack length,  $a$ , is required to ensure that the plastic zone size does not exceed a certain proportion of the crack length, beyond which the 'first term of the series' approximation (needed to derive  $K_c$ ) becomes too inaccurate (Atkins & Mai 1985).

Taking the yield strength as the ultimate tensile strength ( $= 130 \text{ MPa}$ ) and  $K_{Ic}$  as  $4 \text{ MN m}^{-\frac{3}{2}}$ , the minimum dimensions for wet nacre become  $B_{\min} = 2.4 \text{ mm}$ ,  $D_{\min} = 5.9 \text{ mm}$  and  $a_{\min} = 2.4 \text{ mm}$ , which are much larger than those of any test-piece used for wet nacre. The dimensions were not systematically varied between each test so, as a result, there is no significant trend of  $K_c$  with any single dimension.

It is not possible to apply the same criteria to dry nacre because a tensile yield strength (rather than a brittle tensile strength) is not available. If it were anything like the compressive strength ( $450 \text{ MPa}$ ) then the minimum dimensions are satisfied easily. The values of  $K_c$  of dry nacre, and certainly of desiccated nacre, can therefore be safely regarded as plane-strain values.

To partition out the plastic work from the total work of fracture, a line was

drawn parallel to the initial slope of each force-displacement curve and a vertical dropped from the peak load to form a triangle, the area of which represents the elastic fracture energy. Dividing by  $2BD$  then gives a  $G_c$  corrected for plasticity. From this method, plastic work accounts for a maximum of 29% of the total work of fracture of dry nacre and up to 55% of the wet (table 3a).

TABLE 3. CORRECTION FOR PLASTIC WORK IN PINCATA NACRE TESTED IN THREE-POINT BENDING WITH A SINGLE EDGE NOTCH, AND COMPARISON WITH EXPECTED TOUGHNESS

((a) Partitioning of values of  $G_c$  for unstable fracture; (b) partitioning of values of  $G_c$  for stable fracture; (c) correction of values of  $K_c$  for unstable fracture.)

(a)	$S/D$	total $G_c$ $J m^{-2}$	ductility		expected $G_c$ $J m^{-2}$
			corrected $G_c$ $J m^{-2}$	ductility (%)	
across, desiccated	4	264	264	0	7
across, dry	16	352	285	19	290
	4	464	328	29	149
across, wet	16	587	329	44	473
	4	1240	564	55	276
along, dry	11	328	314	4	357
	4	439	417	5	195
along, wet	4	788	614	22	542

(b)	$S/D$	total $G_c$ $J m^{-2}$	ductility		expected $G_c$ $J m^{-2}$
			corrected $G_c$ $J m^{-2}$	ductility (%)	
across, wet	4	889	276	69	276

(c)	$S/D$	original $K_c$ $MN m^{-\frac{3}{2}}$	corrected		expected $K_c$ $MN m^{-\frac{3}{2}}$
			$K_c$ $MN m^{-\frac{3}{2}}$	ductility (%)	
across, desiccated	4	2.9	—	—	?
across, dry	16	4.6	—	—	5.1
	4	3.3	—	—	5.8
across, wet	16	4.5	5.5	18	6.1
	4	3.7	4.2	12	8.9
across, dry	16	5.0	—	—	4.8
	4	3.7	—	—	5.5
along, wet	4	5.0	5.7	12	6.9

Values of  $K_c$  for wet nacre can also be corrected by considering the radius of the plastic zone to be an extension of the actual crack length. Thus

$$K_c = \sigma_f Y \sqrt{\{a(1 + \sigma_f^2/2\sigma_y^2)\}},$$

where  $\sigma_f$  is the nominal flexural strength and  $\sigma_y$  is the yield strength ( $= 130$  MPa) (Knott 1973).

For the same failure stress the addition of this 'embedded crack length' causes an increase in  $K_c$  by about 15% (table 3c). In the absence of a yield strength for dry or desiccated nacre, their values of  $K_c$  have been left uncorrected.

Replotting the values of  $G_c$  corrected for plasticity against the values of  $G_c$  expected from the relation  $K_c^2 = EG_c$ , (with corrected values of  $K_c$  for wet nacre) demonstrates that much of the previous discrepancy was indeed due to plasticity (figure 6). The scatter which remains about the line of equality must be put down to experimental error and inadequacy of the finite-width correction factors for ductile, anisotropic materials. Application of a modified relation between  $K_c$  and  $G_c$  for anisotropic materials (Sih *et al.* 1965) does not improve matters as with  $E_{\text{across}} = E_{\text{along}}$ , and with a shear modulus of about 30 GPa (Srinivasan 1941), the formula reduces approximately to the isotropic case.

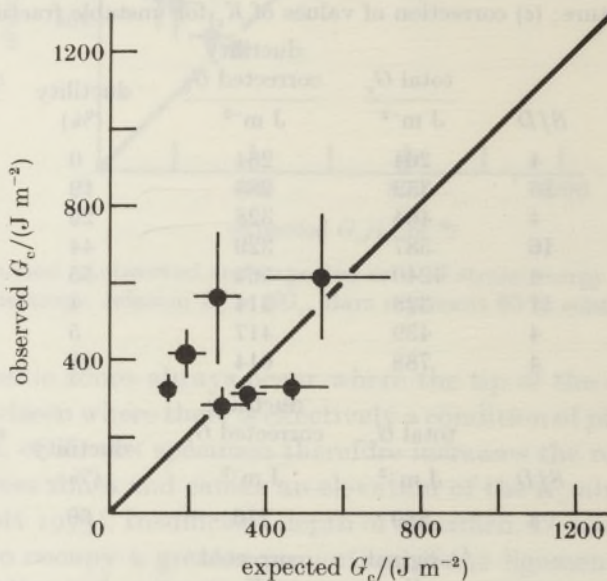


FIGURE 6. Comparison of observed and expected critical strain energy release rates after correction for plasticity. Bars represent 95% confidence limits.

#### DESCRIPTION OF PLATE 1

FIGURES 8–13. Polished surface on the side of a specimen of *Pinctada* nacre tested, wet, in single-edge-notch, three-point bending, in unstable fracture (ratio of span-to-depth = 4).

FIGURE 8. Note the delamination cracks extending laterally from the main crack (accelerating voltage = 30 kV). Scale bar 2.7  $\mu\text{m}$ .

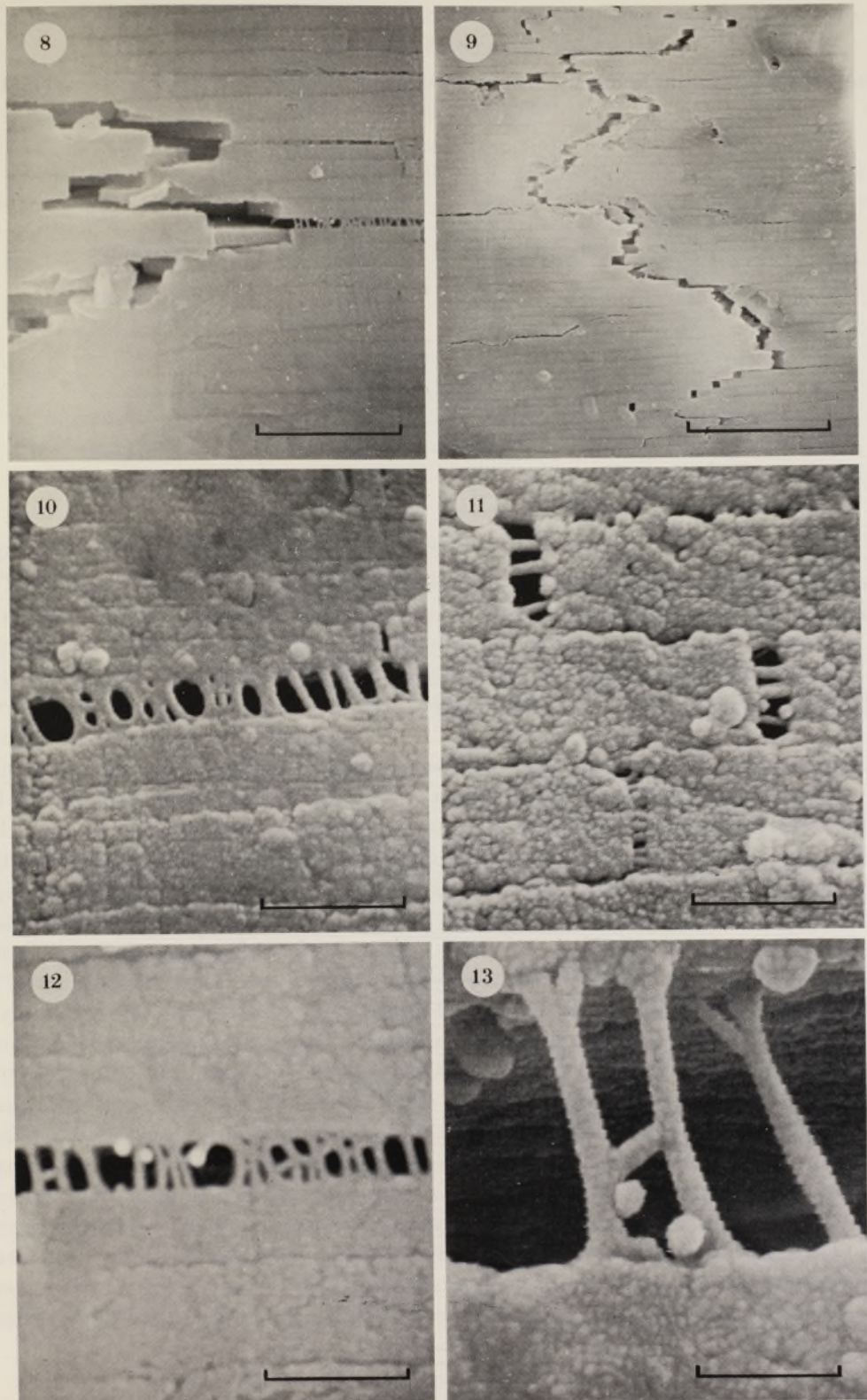
FIGURE 9. Note the delamination cracks just ahead of the main crack tip (accelerating voltage = 30 kV). Scale bar 7.5  $\mu\text{m}$ .

FIGURE 10. Note fibrils of organic matrix bridging the platelet lamellae across a delamination crack (accelerating voltage = 15 kV). Scale bar 0.60  $\mu\text{m}$ .

FIGURE 11. Note fibrils of organic matrix extending between the ends of the platelets where these have been separated in ‘pull-out’ (accelerating voltage = 15 kV). Scale bar 0.43  $\mu\text{m}$ .

FIGURE 12. Note how the fibrils of organic matrix have broken and collapsed back into globules (accelerating voltage = 30 kV). Scale bar 0.60  $\mu\text{m}$ .

FIGURE 13. Fibrils of organic matrix bridging a delamination crack. Note the large extension and ‘splayed-out’ anchorage points. The stepped edges are due to the workings of the SEM and do not convey information about the strands (accelerating voltage = 15 kV). Scale bar 0.20  $\mu\text{m}$ .



FIGURES 8–13. For description see opposite.

(Facing p. 432)

TABLE 4. TOUGHNESS OF *PINCTADA* NACRE IN THREE-POINT BENDING WITH A SINGLE EDGE NOTCH IN STABLE FRACTURE

((a) Continuous propagation method; (b) loading-unloading method (segmental work areas pooled from four specimens).)

(a)	mean work of fracture		number of tests
	J m <sup>-2</sup>	± J m <sup>-2</sup>	
across, dry	437	141	11
across, wet	1034	272	12
along, dry	250	68	9
along, wet	553	167	11

(b)	mean work of fracture		number of segment areas
	J m <sup>-2</sup>	± J m <sup>-2</sup>	
across, wet	889	493	20

#### *Single-edge-notched, three-point bending, stable fracture*

The works of fracture obtained from the first stable crack propagation experiment (table 4a) are in fairly good agreement with those arrived at in the unstable propagation tests. Once again, wet nacre shows superior toughness; however, in contrast to the results of unstable tests, nacre is significantly tougher in the 'across' than in the 'along' direction (wet:  $t(18 \text{ d.f.}) = 3.64$ ,  $0.01 > p > 0.001$ ; dry:  $t(21 \text{ d.f.}) = 5.05$ ,  $p < 0.001$ ).

In the second, stable propagation experiment from three to five cycles of loading and unloading were performed on 4 'across, wet' specimens resulting in 20 replicates of  $R$  that have been pooled together (table 4b). The mean value of  $R$  compares favourably with those from unstable and continuous stable propagation tests. Plastic deformation is manifested in this high value of  $R$ , the nonlinearity of the force-displacement curve, and in the considerable displacement-irreversibility at each loading-unloading cycle.

Plastic fracture work was separated from the total work of fracture by drawing tangents to the initial force-displacement slopes, correcting them for machine compliance, superimposing their origins and joining them up with a straight line at heights corresponding to their peak failure loads (figure 7). Work areas in each triangular segment were then divided by the appropriate area of the crack progression to produce a series of values of  $R$  corrected for ductility (table 3b). It can be seen that irreversible plastic work accounts for about 70% of the total work of fracture and, with this work removed, the value for  $R$  is brought into perfect agreement with what is predicted from the isotropic relation with  $K_c$  and  $E$ . The figures for  $R$  and the ductility-corrected  $R$  values obtained by this method should be regarded as being more trustworthy than those derived using other techniques because no assumptions about linear elasticity or reversibility have been made.

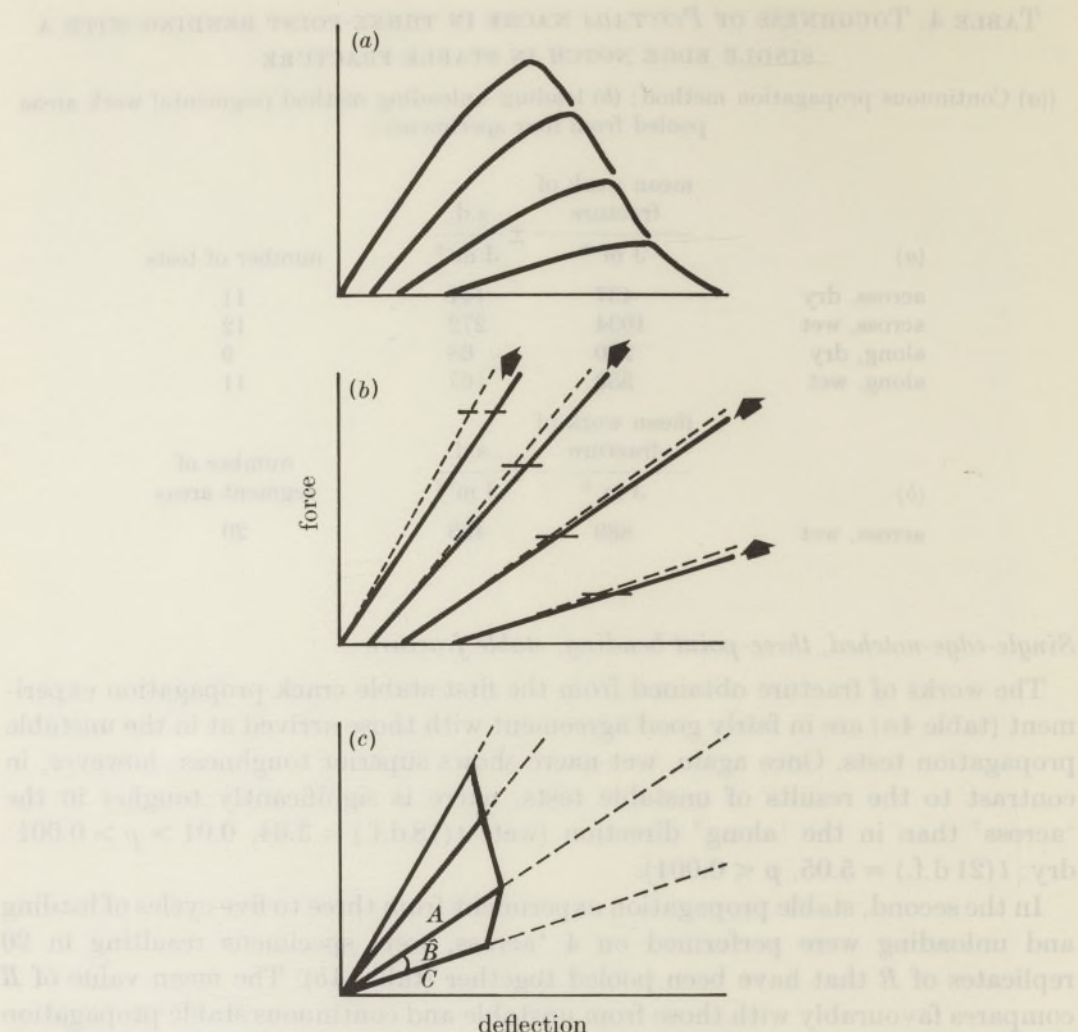


FIGURE 7. The method of correction for ductility in slow propagation, loading-unloading experiments. In (a) are shown the force-deflection curves recorded from the specimen. The initial slope of each curve is taken and a correction made for machine compliance (dotted lines); the peak failure loads from (a) are also marked in (b). In (c) the points denoting peak failure load are joined and the origins of the lines superimposed at the origin. The areas now represent the non-ductile work to fracture (segment area =  $\frac{1}{2}AC \sin \hat{B}$ ).

#### *Analysis of fracture surfaces*

In addition to fracture and pull-out of the platelets, high-resolution SEM revealed a considerable amount of interlamellar debonding in wet nacre, a phenomenon not previously reported for nacre. These delaminations extended laterally down the length of the crack (figure 8, plate 1) and also open up just in front of the crack tip (figure 9, plate 1). They are not associated with any particular mode of crack propagation (i.e. stable or catastrophic), thus ruling out their origin from excess strain energy, and extend to about 0.5 mm away from the crack, corresponding to the region of whitening that can be seen in plastically deformed specimens. The fact that many of the lateral delaminations are isolated from the main crack may

indicate that the intervening lamellae have been healed up owing to the lateral constraint of the surrounding material. Kendall (1981*a, b*) proposed that such 'interfacial dislocations' are responsible for the observed thickness of the lamellae and possibly for the high work of fracture of nacre. Delaminations ahead of the crack tip are probably caused by the component of stress that is perpendicular to the stress concentration responsible for the opening up of the crack (Cook & Gordon 1964). No delaminations (of either variety) could be observed in dry nacre, presumably because of the greater stiffness of the organic matrix.

The final interesting feature to be seen on the fracture surfaces of nacre tested in the across direction is the appearance of the organic matrix. Fibrils of matrix stretch out and bridge the delamination cracks (figure 10, plate 1) and the spaces between the edges of the platelets (figure 11, plate 1). Matrix also adheres to the sides of the delaminations in the form of globules (figure 12, plate 1), which are probably the result of fibrils snapping back on themselves. Other globules occurring on fracture surfaces which go through platelets are assumed to be artefactual. To check that the globules within the delaminations can be reasonably accounted for in this way, the volume of half an extended fibril (assuming it to be cylindrical) was equated with the equivalent volume of a sphere; the diameter of this sphere was then compared with the observed diameter of the collapsed-back globules. With a typical fibril length of 0.4 µm and diameter of 0.04 µm, the expected diameter of a globule is 0.08 µm, which is in fairly good agreement with the observed diameter of the globules of about 0.06 µm. Considering their original coiled-up diameter, the fibrils can stretch out to a remarkable length, equivalent to a strain of 150 %, without becoming detached from the calcium carbonate (figure 13, plate 1).

Bringing together all this information, it is obvious that platelet pull-out is not the only important toughening event during the fracture of nacre. There is large-scale delamination at relatively large distances from the crack tip, provided that the organic matrix is sufficiently hydrated. This damage must surely account for the plastic work during fracture and would explain why plasticity is dependent on *S/D* ratio: debonding between platelet lamellae and the resulting delamination is facilitated by the greater component of shear stress at small *S/D* ratios.

#### *Theoretical modelling*

First, assume that every platelet in the composite is pulled out at the fracture surface. For a composite containing platelets that are perfectly aligned but randomly positioned from one layer to the next, the specific work of fracture is given by

$$R_{\text{pull-out}} = \frac{1}{12} V_p \tau_i t s^2$$

(Piggott 1980).

This was derived by calculating the pull-out energy of a single platelet embedded to a given length, and then integrating the energy over the whole range of embedded lengths.

For nacre, instead of considering a random distribution of embedded lengths, we can assume that the platelets overlap by 50 %. Rather than have to integrate over the whole range of embedded lengths we can now simply sum the work done

by each platelet as it pulls out by a constant amount, equivalent to half its length. The work done in pulling out one platelet is  $wx^2\tau_i$ , where  $w$  is the width of a platelet and  $x$  is the embedded length. If  $N$  is the number of platelets per unit area of cross section being fractured, the predicted work of fracture is now

$$R_{\text{pull-out}} = wL^2\tau_i N,$$

where  $L$  is half the platelet length. Because  $N = V_p/wt$  and  $L^2 = \frac{1}{4}s^2t^2$ , the expression simplifies to

$$R_{\text{pull-out}} = \frac{1}{4}V_p\tau_i ts^2,$$

which is three times larger than the pull-out work of randomly staggered platelets.

It is reasonable to suppose that a work of fracture due to pull-out lies somewhere between the upper limit set by this model and the lower limit set by Piggott's model. Substituting  $V_p = 0.95$ ,  $t = 0.5 \mu\text{m}$ ,  $s = 8$ ,  $\tau_i(\text{dry}) = 46 \text{ MPa}$  and  $\tau_i(\text{wet}) = 37 \text{ MPa}$ , the boundaries on the works of fracture determined by these models are: for dry nacre  $R = 117\text{--}350 \text{ J m}^{-2}$  and for wet nacre  $R = 94\text{--}281 \text{ J m}^{-2}$ . The estimate for dry nacre comes quite close to its measured value (i.e.  $400 \text{ J m}^{-2}$ ) but for wet nacre the work of fracture predicted by even the most generous pull-out model is only 30% of the total measured value (i.e.  $900 \text{ J m}^{-2}$ ).

TABLE 5. TOUGHNESS OF *PINCTADA NACRE*

(Tensile fracture test with a single edge notch, unstable fracture; the specimens were 25 mm between the clamps. Corrections for embedded crack lengths are in parentheses.)

	mean $K_c$ MN m <sup>-3/2</sup>	$\pm$ MN m <sup>-3/2</sup>	s.d. MN m <sup>-3/2</sup>	number of tests
across, dry	3.9	0.8		5
across, wet	4.1 (4.4)	0.7 (0.6)		5
along, dry	5.0	1.0		6
along, wet	4.2 (4.5)	0.7 (0.7)		6

To account for the additional work needed to fracture wet nacre it is necessary to model the contribution from the debonding process during delamination. Outwater & Murphy (1970) showed that the maximum elastic strain energy that can be stored in a platelet is

$$\sigma_{pu}^2(2Lt)y/2E,$$

where  $y$  is the length of platelet over which debonding takes place. Multiplying by the number of platelets per unit area we arrive at

$$R_{\text{debond}} = V_p\sigma_{pu}^2y/2E.$$

There are no precise values for the terms in this equation.  $V_p$  may be safely taken to be 0.95 and  $E_p$  as 100 GPa, but the other two are more difficult to ascertain. For an upper-bound estimate  $\sigma_{pu}^2$  may be guessed to be about 300 MPa (calculated from twice the tensile strength of nacre when  $s = s_c$ ), and from the length of a typical whitened zone in wet nacre,  $y$  is about 1 mm. When these values are put into the above formula,  $R_{\text{debond}}$  emerges at around  $430 \text{ J m}^{-2}$ . Adding it to the upper-bound estimate of pull-out work for wet nacre gives  $R_{\text{total}} = 710 \text{ J m}^{-2}$ .

which is not too far off the observed work of fracture of wet nacre ( $900 \text{ J m}^{-2}$ ). Considering the rather high standard deviations in the measurement of work of fracture and the uncertainty in the estimated parameters, the observed toughness of wet nacre can be explained by a combination of the pull-out and debonding models.

The work of debonding may be augmented by interfacial dislocation. Kendall (1981*a, b*) demonstrated that the modulus and thickness of platelets in nacre are of suitable magnitude in relation to the presumed work of fracture of the interface for the propagation and healing of an interfacial crack to be energetically favourable. Although difficult to quantify, a cycle of debonding and rebonding along interfaces before fracture is a plausible way in which the critical stress concentration may be postponed. It would appear as irreversible (plastic) absorption of energy. But for the mechanism to be analogous to a repetition of the debonding process much energy must be involved, perhaps even as much as is predicted by the Outwater–Murphy debonding model. This being so, some of the conditions of the Outwater–Murphy model that were required to ensure the greatest possible debonding work may now be relaxed. So with both models there is more than enough energy to explain the plastic work term in the fracture toughness of wet nacre.

#### CONCLUSION

The three parameters that have been used to define mechanically a representative form of nacre have been measured successfully by using conventional testing procedures. Water absorbed into the organic matrix of nacre has a significant effect on the Young modulus and tensile strength causing both to be reduced. The most pronounced effect of water is on the work of fracture, causing  $G_c$  of dry nacre to be almost tripled.

The anisotropy of nacre was not fully investigated owing to the difficulty of making measurements in the ‘between’ direction. Very little difference was found in the modulus, strength or toughness of nacre tested in the ‘across’ or ‘along’ directions. Indeed, no difference is to be expected when failure is by pull-out. Not surprisingly, toughness in the ‘between’ direction is considerably lower than in the other two, mutually orthogonal, directions, confirming Currey’s findings.

The absolute values of modulus, strength and toughness of nacre have been predicted quite well by theoretical models which have been applied previously to platey materials whose components are larger in absolute dimensions. Water affects the Young modulus and tensile strength probably by reducing shear modulus and shear strength of the organic matrix. Water affects toughness, probably by plasticizing the organic matrix resulting in a tendency for debonding to occur around the crack tip. This debonding is not a process of brittle fracture but involves the performance of plastic work when the matrix globules bridging the lamellae are drawn into fibrils.

The mechanical properties of nacre in at least three important parameters are explicable in terms of some standard theoretical models. Nacre behaves at the high end of the models’ range and needs a very efficient construction to do so. But with the possible exception of delaminations and interfacial dislocations, nacre does not employ any really novel mechanisms to achieve its mechanical properties.

Nor is nacre perfectly designed in the three parameters that we have looked at. Trivially, nacre does not possess the largest possible Young modulus because it is a composite rather than a pure ceramic but, more importantly, the platelets are below their critical aspect ratio,  $s_c$ . Not only is  $s_c$  optimal for strength but it is also desirable for achieving maximal pull-out work; moreover the increase in  $s$  required to reach  $s_c$  would not be at the expense of a high Young modulus but rather would serve to improve it (cf. the Riley equation).

In the intact mollusc, catastrophic failure is going to be very likely in whole, undamaged shells which behave like unnotched beams at large span-to-depth ratios (Williams 1984). Furthermore, stability is made more difficult by the fact that predators store a lot of strain energy in themselves and operate like 'soft' testing machines. Consequently, the energy that a predator has to put into a shell to cause it to break will be much greater than that predicted by the 'across' work of fracture. When failure does occur it will be lethal to the organism because outer shell materials such as prisms, by all reports, are not sufficiently strong or tough to arrest a fast moving crack. Currey observed crack stopping in nacre, but only by reversing the normal direction of bending (Currey 1977). Because whole shells will normally break catastrophically, what is most important to the organism is not the detail of crack propagation, as Currey implied, but the amount of additional energy absorbed through ductility processes before fracture actually commences.

The effect of structure on the stability of crack propagation in biological materials *in vivo* has not often been pointed out. Absorbing energy during crack propagation may not be an option open to the organism because once the failure load has been reached drastic measures are needed to arrest a crack that is being fed by a large strain energy release rate. This may be the reason why some species of mollusc have sacrificed the high work of fracture of nacre and have opted instead for a strategy whereby cracks can be stopped before it is too late to do repairs. If pieces of broken shell become too widely separated (as they would after catastrophic failure) then it is impossible for the animal to lay down the material from the inside to heal the gap. Molluscs containing crossed-lamellar material, however, have the advantage of a criss-cross arrangement of laths within their shell which enables cracks to be stopped very effectively (Currey & Kohn 1976). Its work of fracture is unlikely to be as high as that of nacre because there are fewer reinforcing elements per cross-sectional area available for pull-out, yet this might be a small price to pay for the sake of having the ability to arrest cracks.

It has been shown that the amount of ductility increases at smaller  $S/D$  ratios and a possible source of  $S/D$ -dependent ductility is investigated. For the nacre-bearing mollusc this has strong repercussions on the vulnerability of long, thin shells as opposed to short, thick ones. If, for example, shells grow more in length than in thickness then young shells with effectively small  $S/D$  ratios should be more ductile and able to absorb more energy per unit mass of shell than old ones. As yet we have no evidence for this.

This work was supported by a SERC CASE award in collaboration with ICI plc Wilton Materials Research Centre. We are grateful to Dr G. Jeronimidis,

Professor A. G. Atkins, Professor J. G. Williams, Professor E. H. Andrews, Dr J. Behiri and Professor J. D. Currey for advice and to Professor Currey for extensive comments on the paper. The scanning electron micrographs appear by courtesy of Mr R. Crick of ICI plc. The Instron materials testing machine was bought with a grant from the Royal Society.

## REFERENCES

- Addadi, L. & Weiner, S. 1985 Interactions between acidic proteins and crystals: stereochemical requirements in biomineralization. *Proc. natn. Acad. Sci. U.S.A.* **82**, 4110–4114.
- American Society for Testing and Materials 1976 Standard test method for apparent inter-laminar shear strength of parallel fiber composites by short beam method. *ASTM D2344*.
- Atkins, A. G. & Mai, Y.-W. 1985 *Elastic and plastic fracture*: metals, polymers, ceramics, composites, biological materials. Chichester: Ellis-Horwood.
- Bilby, B. A., Cottrell, A. H. & Swinden, K. H. 1963 The spread of plastic yield from a notch. *Proc. R. Soc. Lond. A* **272**, 304–314.
- Brown, W. F. & Srawley, J. E. 1966 *Plane strain crack testing of high strength metallic materials*. ASTM Special Technical Publication no. 410.
- Chen, P. E. & Lewis, T. B. 1970 Stress analysis of ribbon reinforced composites. *Polym. Engng Sci.* **10**, 43–47.
- Cook, J. & Gordon, J. E. 1964 A mechanism for the control of crack propagation in all-brittle systems. *Proc. R. Soc. Lond. A* **282**, 508–520.
- Cox, H. L. 1952 The elasticity and strength of paper and other fibrous materials. *Br. J. appl. Phys.* **3**, 72–79.
- Currey, J. D. 1977 Mechanical properties of mother of pearl in tension. *Proc. R. Soc. Lond. B* **196**, 443–463.
- Currey, J. D. 1980 Mechanical properties of mollusc shell. In *The mechanical properties of biological materials (Symp. Soc. exp. Biol. 34)* (ed. J. F. V. Vincent & J. D. Currey), pp. 75–97. Cambridge University Press.
- Currey, J. D. & Brear, K. 1984 Fatigue fracture of mother-of-pearl and its significance for predatory techniques. *J. Zool.* **204**, 541–548.
- Currey, J. D. & Kohn, A. J. 1976 Fracture in the crossed-lamellar structure of *Conus* shells. *J. Mater. Sci.* **11**, 1616–1623.
- Currey, J. D. & Taylor, J. D. 1974 The mechanical behaviour of some molluscan hard tissues. *J. Zool.* **173**, 395–406.
- Glavinchevski, B. & Piggott, M. 1973 Steel disc reinforced polycarbonate. *J. Mater. Sci.* **8**, 1373–1382.
- Greenfield, E. M., Wilson, D. C. & Crenshaw, M. A. 1984 Ionotropic nucleation of calcium carbonate by molluscan matrix. *Am. Zool.* **24**, 925–932.
- Harris, B. 1980 The mechanical behaviour of composite materials. In *The mechanical properties of biological materials (Symp. Soc. exp. Biol. 34)* (ed. J. F. V. Vincent & J. D. Currey), pp. 37–74. Cambridge University Press.
- Hashemi, S. & Williams, J. G. 1984 Size and loading effects in fracture toughness testing of polymers. *J. Mater. Sci.* **19**, 3746–3759.
- Hearmon, R. F. S. 1946 The elastic constants of anisotropic materials. *Rev. mod. Phys.* **18**, 409–440.
- Hull, D. 1981 *An introduction to composite materials*. Cambridge University Press.
- Jackson, A. P. 1986 The mechanical design of nacre. Ph.D. thesis, University of Reading.
- Jackson, A. P., Vincent, J. F. V., Briggs, D., Crick, R. A., Davies, S. F., Hearn, M. J. & Turner, R. M. 1987 The application of surface analytical techniques to the study of fracture surfaces in mother-of-pearl. *J. Mater. Sci. Lett.* **5**, 975–978.
- Kendall, K. 1981a Interfacial dislocations in tough adhesive composites. *Phil. Mag. A* **43**, 713–729.

- Kendall, K. 1981b Dislocations at adhesive interfaces in composites. *Int. J. Adhesion Adhesives* **1**, 301–304.
- Kitchener, A. C. 1985 The functional design of horns. Ph.D. thesis, University of Reading.
- Knott, J. F. 1973 *Fundamentals of fracture mechanics*. London: Butterworths.
- Krampitz, G., Drolshagen, H., Hausle, J. & Hof-Irmscher, K. 1983 Organic matrices of mollusc shells. In *Biomineralization and biological metal accumulation* (ed. P. Westbroek & E. W. de Jong), pp. 231–247. Dordrecht: Reidel.
- Lusis, J., Woodhams, R. T. & Xanthos, M. 1973 The effect of flake aspect ratio on the flexural properties of mica reinforced plastics. *Polym. Engng Sci.* **13**, 139–145.
- McGee, S. & McCullough, R. L. 1981 Combining rules of predicting the thermoelastic properties of particulate filled polymers, polyblends and foams. *Polym. Composites* **2**, 149–161.
- Outwater, J. O. & Murphy, M. C. 1970 Fracture energy of unidirectional laminates. *Mod. Plast.* **47**, 160–169.
- Padawer, G. E. & Beecher, N. 1970 On the strength and stiffness of planar reinforced plastic resins. *Polym. Engng Sci.* **10**, 185–192.
- Piggott, M. R. 1980 *Load bearing fibre composites*. Oxford: Pergamon Press.
- Riley, V. R. 1968 Fibre/fibre interaction. *J. comp. Mater.* **2**, 436–446.
- Roark, R. J. & Young, W. C. 1975 *Formulas for stress and strain*, 5th edn. London: MacGraw-Hill International.
- Sih, G. C., Paris, P. C. & Irwin, G. R. 1965 On cracks in rectilinearly anisotropic bodies. *Int. J. Fract. Mech.* **1**, 189–203.
- Srinivasan, P. S. 1941 The elastic properties of molluscan shells. *Q. Jl Ind. Inst. Sci.* **4**, 189–221.
- Stephens, R. C. 1970 *Strength of materials: theory and examples*. London: Edward Arnold.
- Wagner, H. D., Fischer, S., Roman, I. & Marom, G. 1981 The effect of fibre content on the simultaneous determination of Young's and shear moduli of unidirectional composites. *Composites* **12**, 257–259.
- Wainwright, S. A., Biggs, W. D., Currey, J. D. & Gosline, J. M. 1976 *Mechanical design in organisms*. London: Edward Arnold.
- Weiner, S. & Traub, W. 1981 Organic matrix–mineral relationships in mollusk shell nacreous layers. In *Structural aspects of recognition and assembly in biological macromolecules* (ed. M. Balban, J. L. Sussman, W. Traub & A. Yonath), pp. 467–482. Philadelphia: Rehovot.
- Williams, J. G. 1984 *Fracture mechanics of polymers*. Chichester: Ellis Horwood.
- Zweben, C., Smith, W. S. & Wardle, M. W. 1979 Test methods for fiber tensile strength, composite flexural modulus and properties of fabric-reinforced laminates. In *Composite materials: testing and design (5th conference)* (ed. S. W. Tsai), pp. 244–262. ASTM special publication 674.